

# Orthogonalized Policy Optimization

Decoupling Sampling Geometry from Optimization Geometry in RLHF

Wang Zixian

China Mobile Communications Group Shandong Co., Ltd. Tai'an Branch

wangzixian@sd.chinamobile.com

## Abstract

Large Language Model (LLM) alignment objectives are often presented as a collection of distinct algorithms—PPO, DPO, IPO, and their variants—each motivated by different derivations. In this work, we argue that this diversity obscures a simpler underlying structure. At a fundamental level, alignment objectives involve two independent design choices: (i) *how training signals are sampled and weighted*, and (ii) *how deviations from a reference policy are geometrically penalized*. Existing methods typically entangle these choices through a single divergence, most commonly the Kullback–Leibler (KL) divergence.

We show that this entanglement is not merely a modeling convenience but a source of systematic instability. When the same divergence simultaneously determines sample weighting and optimization curvature, adjusting one aspect (e.g., exploration strength) inevitably alters the other (e.g., gradient geometry). This coupling is particularly problematic in preference-based reinforcement learning, where advantage signals are unbounded and high-confidence regimes are common.

We propose a simple but structural remedy: formulate alignment as an *orthogonal mirror descent* problem, in which sampling geometry enters only as a linear driving force, while optimization geometry is determined independently by a mirror map. This perspective leads to a new alignment objective—**Orthogonalized Policy Optimization (OPO)**—obtained by choosing a Euclidean mirror map in likelihood-ratio space. The resulting objective admits a closed-form solution, linear (non-saturating) gradient dynamics, and a well-conditioned trust region, while remaining fully compatible with standard LLM training pipelines.

## 1 Introduction

Aligning Large Language Models (LLMs) with human preferences has become a cornerstone of modern AI development. The standard paradigm, Reinforcement Learning from Human Feedback (RLHF) [5, 6], typically employs algorithms like Proximal Policy Optimization (PPO) [2] or Direct Preference Optimization (DPO) [1] to optimize a policy against a reward model or preference dataset. Despite their formulation differences, these methods share a common structural foundation: they all rely on Kullback–Leibler (KL) divergence to constrain the policy update, preventing it from deviating excessively from a reference distribution.

While empirically effective, KL-regularized objectives exhibit distinct limitations in reasoning-intensive domains where high confidence is required. As the policy improves and assigns high probability to correct reasoning chains, the KL penalty—which induces an exponential geometry in the log-probability space—often dominates the learning signal. This manifests as gradient saturation, where the driving force for further improvement vanishes exponentially as the model becomes confident. Consequently, training often plateaus prematurely, behavior commonly attributed to "over-regularization" but which we argue is intrinsic to the chosen geometry.

We contend that this issue stems from a structural conflation in existing objective designs. Fundamentally, alignment involves two independent design choices: *sampling geometry*, which determines the effective weighting of training examples (e.g., whether to focus on high-advantage samples), and *optimization geometry*, which determines the curvature of the update step (e.g., how to measure distance

in the policy space). In standard KL-based methods, a single divergence term dictates both, coupling the exploration strength with the optimization stability. Adjusting one inevitably perturbs the other, creating a dilemma where aggressive sampling destabilizes training, while stable optimization stifles exploration.

To resolve this, we propose a unifying framework based on **Orthogonal Mirror Descent**. By viewing alignment as a mirror descent process, we can explicitly decouple these two axes: the sampling geometry acts as a linear driving force defined by an advantage-weighted distribution, while the optimization geometry is independently governed by a Bregman divergence (mirror map). This perspective reveals that the saturation observed in DPO and PPO is not a necessary feature of alignment, but a specific consequence of using the Negative Entropy mirror map (which induces KL divergence).

Guided by this framework, we introduce **Orthogonalized Policy Optimization (OPO)**, a new alignment objective derived by selecting the *Euclidean mirror map* in the space of likelihood ratios. Unlike the exponential geometry of KL, the Euclidean geometry induces a Pearson  $\chi^2$  trust region, leading to a quadratic regularizer that maintains a linear, non-saturating driving force even in high-confidence regimes. This formulation cleanly separates the sampling intensity (controlled by an  $\alpha$ -divergence parameter) from the regularization strength (controlled by a stiffness parameter), allowing for robust, continuous improvement.

Our contributions are as follows:

- We identify the implicit coupling of sampling and optimization geometries in KL-based alignment methods as a root cause of gradient saturation.
- We propose the Orthogonal Mirror Descent framework, which theoretically decouples these design axes.
- We derive Orthogonalized Policy Optimization (OPO), a simple, closed-form objective based on Euclidean geometry that ensures linear gradient dynamics and global contraction.
- We empirically demonstrate that OPO outperforms strong baselines like DPO and GRPO on mathematical reasoning tasks, validating the benefits of non-saturating gradients.

## 2 Related Work

**Preference Optimization and RLHF.** Reinforcement Learning from Human Feedback (RLHF) typically involves learning a reward model from preferences and then optimizing a policy via PPO [2, 5, 6]. Direct Preference Optimization (DPO) [1] simplifies this by deriving a closed-form solution to the KL-constrained reward maximization problem. Recent variants extend this paradigm: IPO [7] adds a regularization term to prevent overfitting, SimPO [8] simplifies the reference-free objective.

**$f$ -Divergences in Machine Learning.** The  $f$ -divergence family [9, 10] provides a unified framework for measuring distributional discrepancy. The Csiszár–Amari  $\alpha$ -divergence [9, 11] continuously connects forward and reverse KL. Prior work has explored  $f$ -divergences in variational inference [12], GANs [13], and imitation learning [14]. In RL,  $\alpha$ PPO [15] studied  $\alpha$ -divergence as a trust-region constraint. Recently, APO [16] explored combining forward and reverse KL dynamics for standard preference optimization. OPO builds on these foundations by decomposing the divergence into independent geometry axes.

**Trust-Region Methods.** TRPO [3] enforces stability via explicit KL constraints, while PPO [2] approximates this with ratio clipping. ADPO [17] shows that anchored coordinates provide an implicit trust region via temperature-scaled curvature. OPO extends this by replacing the KL-based geometry with a quadratic ( $\chi^2$ ) geometry in ratio coordinates, providing a different form of implicit regularization.

### 3 Theoretical Framework: Two Independent Design Axes

We formalize the OPO framework by decomposing the alignment objective into two orthogonal components.

#### 3.1 Coordinates: Ratio Space vs. Log-Ratio Space

Let the reference policy be  $\pi_{\text{ref}}$ . We define two coordinate systems for measuring policy deviation:

**Definition 3.1** (Ratio Coordinates). The *density ratio* and *centered ratio* are:

$$t_\theta(y) := \frac{\pi_\theta(y)}{\pi_{\text{ref}}(y)}, \quad v_\theta(y) := t_\theta(y) - 1 = \frac{\pi_\theta(y)}{\pi_{\text{ref}}(y)} - 1 \quad (1)$$

**Definition 3.2** (Log-Ratio Coordinates). The *log-ratio* (natural parameterization of LLMs) is:

$$\Delta_\theta(y) := \log \pi_\theta(y) - \log \pi_{\text{ref}}(y) \quad (2)$$

so that  $t_\theta(y) = \exp(\Delta_\theta(y))$  and  $v_\theta(y) = \exp(\Delta_\theta(y)) - 1$ .

The key observation is that  $\chi^2$  divergence is naturally quadratic in ratio coordinates  $v$ , while KL divergence involves the log-ratio  $\Delta$ . This distinction is crucial for understanding the gradient dynamics of different alignment objectives.

### 4 Theoretical Framework: Orthogonal Mirror Descent

We present a unified framework that fundamentally decouples the *preference sampling geometry* (what to learn) from the *optimization geometry* (how to learn). We formulate policy alignment as a functional **Orthogonal Mirror Descent** problem.

#### 4.1 The General Framework

We view alignment as an iterative projection process. At each step  $k$ , we seek a policy  $\pi$  that maximizes the expected return under a specific sampling distribution  $\rho_\alpha$ , subject to a trust-region constraint defined by a divergence  $D_\Psi$ :

$$\pi_{k+1} = \arg \max_{\pi} \mathbb{E}_{y \sim \rho_\alpha} [A(y) \log \pi(y)] - \frac{1}{\eta} D_\Psi(\pi \| \pi_k) \quad (3)$$

This formulation cleanly orthogonizes two design axes:

1. **Sampling Geometry** ( $\rho_\alpha$ ): Determines the effective weighting of samples (the linear driving force).
2. **Optimization Geometry** ( $D_\Psi$ ): Determines the mirror map (regularization/curvature) used to project the update.

#### 4.2 Axis 1: Sampling Geometry Specification

The sampling distribution  $\rho_\alpha$  controls the exploit-explore tradeoff in the data. We define the preference weight  $\omega_\alpha(y)$  generally as an  $\alpha$ -parameterized linear signal that reweights the advantage  $A(y)$ .

$$\omega_\alpha(y) \propto \text{Projection}_\alpha(A(y), \pi_{\text{ref}}(y)) \quad (4)$$

Specific constructions include the  $\alpha$ -divergence optimal target or other heavy-tailed reweighting schemes. This explicit definition avoids ambiguity:  $\omega_\alpha$  represents the abstract "force" pulling the policy towards high-reward regions, decoupled from the optimization dynamics.

### 4.3 Axis 2: Optimization Geometry: Euclidean Mirror Map

The core innovation of OPO is the choice of the mirror map. Instead of the standard Negative Entropy map (which leads to KL divergence and exponential updates), we choose the **Euclidean Mirror Map** in the space of likelihood ratios  $v = \pi/\pi_{\text{ref}} - 1$ :

$$\Psi(v) = \frac{1}{2} \|v\|_{L^2(\pi_{\text{ref}})}^2 = \frac{1}{2} \mathbb{E}_{y \sim \pi_{\text{ref}}} [v(y)^2] \quad (5)$$

The induced Bregman divergence is the Pearson  $\chi^2$  divergence:

$$D_{\Psi}(\pi\|\pi_k) = \frac{1}{2} \mathbb{E}_{\pi_{\text{ref}}} \left[ \left( \frac{\pi}{\pi_{\text{ref}}} - \frac{\pi_k}{\pi_{\text{ref}}} \right)^2 \right] = D_{\chi^2}(\pi\|\pi_k) \quad (6)$$

This choice transforms the alignment problem into a quadratic optimization in ratio space.

### 4.4 Orthogonalized Policy Optimization (OPO)

Substituting the Euclidean geometry into our framework yields the OPO objective:

$$\mathcal{L}_{\text{OPO}} = -\mathbb{E}_{y \sim \pi_{\text{ref}}} [\omega_{\alpha}(y) v(y)] + \frac{\mu}{2} \mathbb{E}_{y \sim \pi_{\text{ref}}} [v(y)^2] \quad (7)$$

where  $\mu = 1/\eta$  is the stiffness parameter. The solution is available in closed form:  $v^*(y) = \omega_{\alpha}(y)/\mu$ .

*Remark 4.1* (Analogy with Quantum Amplitudes). A physical analogy elucidates the advantages of the Euclidean geometry.

- **Ratio Space as Amplitude:** In quantum mechanics, superpositions are linear in *amplitude* ( $\psi$ ). Similarly, OPO operates in the ratio space  $v$ , allowing preference signals to superpose linearly without saturation.
- **KL Space as Probability:** KL-based methods operate in *log-probability* space. Analogous to adding energies in a Boltzmann distribution, this enforces exponential scaling, which leads to "probability collapse" or saturation when signals are strong.

By working in "amplitude" (ratio) space with quadratic "energy" (regularization), OPO maintains a non-saturating linear response field, crucial for long-chain reasoning where we must avoid premature collapse to a single path.

### 4.5 Log-Ratio Approximation

For implementation in LLMs (which output logits), we use the log-ratio  $\Delta_{\theta} = \log \pi_{\theta} - \log \pi_{\text{ref}}$ . As shown in Appendix A, for small trust regions,  $v \approx \Delta$ .

$$\mathcal{L}_{\text{OPO}}^{\log} \approx - \sum_{y \in S} \omega_{\alpha}(y) \Delta_{\theta}(y) + \frac{\mu}{2} \mathbb{E}_{\pi_{\text{ref}}} [\Delta_{\theta}(y)^2] \quad (8)$$

This retains the linear dynamics of the Euclidean geometry while remaining compatible with standard gradient-based training.

*Remark 4.2* (On-Policy Anchoring). We set  $\pi_{\text{ref}} = \pi_{\text{old}}$  (on-policy anchoring), ensuring the trust region condition  $\Delta \approx 0$  holds locally, justifying the approximation.

## 4.6 Gradient Dynamics

For the ratio-coordinate objective Equation (7), the gradient w.r.t.  $v_\theta(y)$  is:

$$\nabla_v \mathcal{L}_{\text{OPO}}^{\text{ratio}} = -\omega_\alpha(y) + \mu v_\theta(y) \quad (9)$$

with the unique equilibrium:

$$v^*(y) = \frac{\omega_\alpha(y)}{\mu} \quad (10)$$

This linear relationship has several desirable properties:

1. **Stable Equilibrium:** The objective is strictly convex in  $v_\theta(y)$  for fixed  $\omega_\alpha(y)$ , yielding a unique stationary point in the ratio coordinate.
2. **No Saturation:** Unlike sigmoid-based losses, the gradient magnitude does not vanish as  $v$  grows.
3. **Orthogonal Control:** Changing  $\alpha$  (sampling) affects only  $\omega_\alpha$ ; changing  $\mu$  (optimization) affects only the regularization strength. The two do not interact.

## 5 Theoretical Analysis

We formalize the decoupling of design axes and analyze the distinct regularization properties of OPO.

### 5.1 Decoupled Sampling and Optimization Geometry

We analyze the optimization dynamics in the *function space of ratio outputs*  $v$ . This perspective captures the intrinsic objective geometry. We first formalize the connection to parameter space dynamics.

**Lemma 5.1** (Parameter Space Gradient Projection). *Let  $\mathcal{L}(v_\theta)$  be a functional of the policy output  $v_\theta(y)$ . The gradient in parameter space  $\theta$  is the projection of the function-space gradient  $\nabla_v \mathcal{L}$  onto the tangent space of the policy manifold:*

$$\nabla_\theta \mathcal{L}(\theta) = \mathbb{E}_{y \sim \pi_{\text{ref}}} [\nabla_v \mathcal{L}(v_\theta(y)) \cdot \nabla_\theta v_\theta(y)] \quad (11)$$

Thus, the geometric properties of  $\nabla_v \mathcal{L}$  directly determine the driving force in parameter space, modulated by the policy's local sensitivity  $\nabla_\theta v_\theta$ .

With this link established, we characterize the geometry of  $\mathcal{L}(v)$ .

**Theorem 5.2** (Decoupled Sampling and Optimization Geometry). *Consider the OPO objective  $\mathcal{L}(v) = -\sum_y \omega_\alpha(y)v(y) + \frac{\mu}{2}\mathbb{E}_{\pi_{\text{ref}}}[v(y)^2]$ . In the space of ratio functions  $v \in L^2(\pi_{\text{ref}})$ :*

1. *The first-order driving force depends on the sampling parameter  $\alpha$ :*

$$\nabla_v \mathcal{L} = -\omega_\alpha(y) + \mu v(y) \quad (12)$$

2. *The second-order curvature is independent of  $\alpha$ :*

$$\nabla_v^2 \mathcal{L} = \mu I \quad (13)$$

*Proof.* Direct differentiation yields a constant Hessian  $\mu I$ , which is independent of  $\alpha$ .

This structural decoupling guarantees stable, predictable convergence dynamics in the function space.

**Corollary 5.3** (Global Contraction and Linear Convergence). *Gradient descent in  $v$ -space on the OPO objective follows a linear dynamical system:*

$$v_{k+1} - v^* = (1 - \eta\mu)(v_k - v^*) \quad (14)$$

where  $v^* = \omega_\alpha/\mu$ . For step size  $0 < \eta < 2/\mu$ , this system exhibits **global contraction** to the unique equilibrium. The contraction rate  $|1 - \eta\mu|$  depends solely on the optimization stiffness  $\mu$ , confirming that convergence speed is structurally decoupled from the target distribution sharpness  $\alpha$ .

We use the term “orthogonalized” to emphasize this control decoupling.

**Remark 5.4** (Contrast with KL-Based Methods). In KL-regularized objectives (e.g., DPO), the effective loss locally resembles a logistic function  $\mathcal{L} \approx -\log \sigma(\text{margin})$ . The *local curvature* scales as  $\beta^2 \sigma(m)(1 - \sigma(m))$ , where  $m$  is the logit margin. This curvature depends on both the temperature  $\beta$  and the current data margin  $m$ . Thus, changing  $\beta$  simultaneously alters both the gradient magnitude and the local stability profile, entangling the two design axes. OPO’s constant curvature  $\mu$  avoids this data-dependent instability.

## 5.2 Comparison with Parametric L2 Regularization

A natural question is whether OPO differs fundamentally from standard Policy Gradient with L2 parameter regularization (weight decay).

$$\mathcal{L}_{\text{L2-PG}} = -\mathbb{E}[A \log \pi_\theta] + \frac{\lambda}{2} \|\theta - \theta_0\|^2 \quad (15)$$

While both methods induce a quadratic penalty, they operate in fundamentally different spaces:

1. **Functional vs. Parametric Prior:** OPO’s penalty  $\frac{\mu}{2} \mathbb{E}[v^2]$  acts in the *function space* of probability ratios. It penalizes deviations only where the policy assigns probability mass. L2 parameter regularization acts in the *weight space*. Two different policies can have the same L2 distance, and small weight changes can cause large output deviations (and vice-versa).
2. **Adaptive Constraint:** OPO’s regularization provides a “linear restoring force” directly on the probability ratio. If the model is confident (large  $v$ ), the  $\chi^2$  penalty generates a strong, specific gradient signal to pull *that specific output* back. Parametric L2 is blind to the output; it uniformly decays all weights regardless of their contribution to the current output confidence.
3. **Learning Dynamics:** Empirically, Functional  $\chi^2$  regularization allows the model to shift mass aggressively where advantages are high, while maintaining stability. Weight decay suppresses all weight magnitudes, which can inadvertently hinder the learning of sharp, high-confidence reasoning chains required for math tasks.

## 5.3 Quantitative Gradient Analysis

We provide a quantitative comparison of the gradient signal in high-confidence regimes, proving the non-saturation property.

**Gradient Saturation in DPO.** For logistic-based losses (DPO), the gradient magnitude with respect to the margin  $m$  is  $|\nabla_m \mathcal{L}| = |\beta \sigma(m)(1 - \sigma(m))|$ . Since  $\sigma(1 - \sigma) \leq 1/4$ :

$$|\nabla_{\text{DPO}}| \leq \frac{\beta}{4} \quad (16)$$

Crucially, as the margin  $m \rightarrow \infty$ ,  $|\nabla_{\text{DPO}}| \rightarrow 0$  exponentially.

**Linear Gradient Dynamics in OPO.** For OPO, the gradient is  $\nabla_v \mathcal{L} = \mu v - \omega_\alpha$ . Let  $v^* = \omega_\alpha/\mu$ . The gradient magnitude is exactly proportional to the distance from equilibrium:  $|\nabla_v \mathcal{L}| = \mu|v - v^*|$ . Therefore, for any non-equilibrium state ( $|v - v^*| \geq \delta$ ):

$$|\nabla_{\text{OPO}}| \geq \mu\delta \quad (17)$$

This guarantees a linear driving force that does not vanish arbitrarily, preventing the saturation observed in KL-based methods.

## 5.4 Algorithm and Flowchart

We provide a visual overview of the OPO process in Figure 1 and the detailed procedure in Algorithm 2.

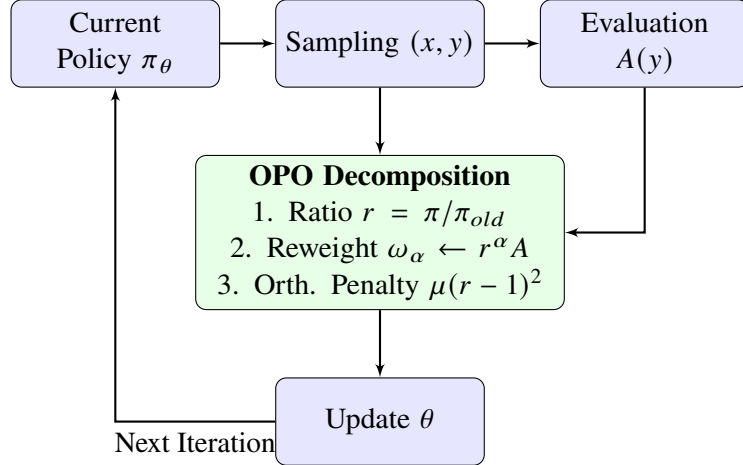


Figure 1: Flowchart of the Orthogonalized Policy Optimization (OPO) framework. The core innovation lies in the “OPO Decomposition” block (green), which separates the advantage signal (reweighted by  $\alpha$ ) from the trust-region constraint (quadratic penalty  $\chi^2$ ), ensuring linear non-saturating gradients.

### Algorithm 1: Orthogonalized Policy Optimization (OPO)

**Input:** Initial policy  $\pi_\theta$ , hyperparameters  $\alpha, \mu, \eta$

**for** each iteration **do**

1. **Set Reference:**  $\pi_{\text{ref}} \leftarrow \pi_\theta$  *(on-policy anchoring)*
2. **Collect Rollouts:** Sample  $(x, y) \sim \pi_\theta$ , compute rewards  $R(x, y)$
3. **Compute Advantages:**  $A(y) \leftarrow R(y) - \bar{R}$  *(group-normalized)*
4. **Compute Weights:**  $\omega_\alpha(y) \leftarrow A(y) \cdot [\text{reweight by } \alpha]$  *(sampling geometry)*
5. **Compute Ratio:**  $v_\theta(y) \leftarrow \pi_\theta(y)/\pi_{\text{ref}}(y) - 1$  *(or use log-approx)*
6. **Compute Loss:**  $\mathcal{L} \leftarrow -\sum_y \omega_\alpha(y)v_\theta(y) + \frac{\mu}{2} \sum_y v_\theta(y)^2$  *(optimization geometry)*
7. **Update Policy:**  $\theta \leftarrow \theta - \eta \nabla_\theta \mathcal{L}$

**end for**

Figure 2: Pseudocode for Orthogonalized Policy Optimization. The algorithm explicitly decouples sampling geometry (step 4) from optimization geometry (step 6).

## 6 Experiments

We conduct an empirical comparison of OPO against three strong baselines—GRPO, GSPO, and DAPO—on mathematical reasoning tasks using the VERL framework.

### 6.1 Experimental Setup

**Model and Data.** We use Qwen3-1.7B as the base model and train on MATH Level 3 problems. All methods use identical training configurations: 4 epochs, batch size 32, learning rate  $2 \times 10^{-6}$ , and 6 rollout generations per prompt.

#### Baseline Configurations.

- **GRPO** (Group Relative Policy Optimization) [4]: Standard token-level policy gradient with group-normalized advantages. Uses vanilla PPO loss mode without a value function critic.
- **GSPO** (Group Sentence-level Policy Optimization): A variant of GRPO that applies advantage normalization at the sentence/step level rather than the token level, aiming for more granular credit assignment.
- **DAPO** (Dynamic Advantage Policy Optimization): An advanced baseline incorporating four key mechanisms:
  1. **Clip Higher**: Raises the PPO clip upper bound (e.g.,  $1 + \epsilon \rightarrow 1.28$ ) to mitigate entropy collapse and preserve exploration.
  2. **Dynamic Sampling**: dynamically filters "all-correct" or "all-wrong" samples that contribute zero advantage, focusing training on informative samples.
  3. **Token-Level Policy Gradient**: Standardizes advantage weights across tokens in a mini-batch to prevent gradient dilution in long sequences.
  4. **Overlong Reward Shaping**: Applies a length-aware penalty and masks gradients for truncated responses to reduce noise.
- **OPO**: The proposed method with  $\alpha = 0.6$ ,  $\mu = 1.0$ , on-policy anchoring ( $\pi_{\text{ref}} = \pi_{\text{old}}$ ), and adaptive  $\tau$  with range  $[0.2, 1.5]$ .

### 6.2 Results

**Overall Performance.** Table 1 summarizes the key metrics across all four algorithms.

Table 1: Comparison of alignment algorithms on Qwen3-1.7B + MATH Level 3. Reward and gradient norm are averaged over the final 20 training steps.

Algorithm	Mean Reward	Grad Norm	Characteristics
GRPO	0.686	0.61	Standard baseline, stable
GSPO	0.713	0.50	Strong, some gradient decay
DAPO	0.67*	0.22	Conservative, early plateau
<b>OPO (Ours)</b>	<b>0.756</b>	<b>0.90</b>	Best reward, non-saturating gradients

## Algorithm Characteristics.

- **GRPO**: Serves as the canonical baseline. Achieves reasonable performance (69% acc) with moderate gradient norms. The token-level normalization provides stability but may average out strong signals.
- **GSPO**: Improves upon GRPO (71% acc) via sentence-level credit assignment. However, gradient norms (0.50) are lower than OPO’s, suggesting some saturation in high-confidence regimes.
- **DAPO**: Exhibits the lowest gradient norms (0.22) and plateaus early. The conservative clipping constraints appear overly restrictive for reasoning tasks where continued learning is beneficial.  
\*Note: Reward fluctuated between 0.59–0.67.
- **OPO**: Achieves the highest mean reward (0.756) while maintaining the largest gradient norms (0.90). This empirically validates the theoretical prediction: the  $\chi^2$  geometry provides non-saturating linear gradients, allowing the model to continue learning where others plateau.

**Training Dynamics.** Figure 3 shows the training accuracy (mean reward) over 224 training steps.

- **Early Stage**: GRPO exhibits the fastest initial learning, surpassing OPO in the first 50 steps. This is consistent with standard policy gradient methods having aggressive early updates.
- **Late Stage Cross-over**: As training progresses (after step 100), GRPO and GSPO begin to saturate. In contrast, OPO maintains a steady improvement rate, eventually overtaking all baselines to reach the highest final accuracy (~76%). This confirms that the  $\chi^2$ -induced linear drive prevents the “vanishing gradient” problem common in KL-constrained methods as confidence increases.

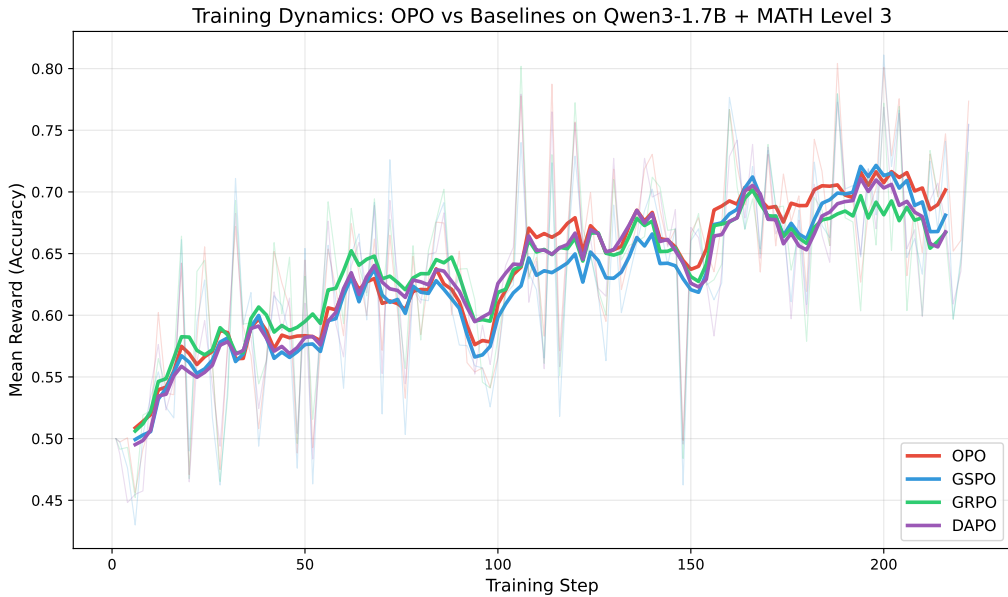


Figure 3: Training dynamics on Qwen3-1.7B Math RL. Note the cross-over behavior: GRPO (green) starts strong but plateaus, while OPO (red) sustains improvement and achieves the highest final performance.

**Gradient Behavior.** Figure 4 illustrates the gradient norm dynamics across training. OPO exhibits consistently higher gradient norms, validating the non-saturating property of the  $\chi^2$  geometry. DAPO shows severely diminished gradients, explaining its early plateau.

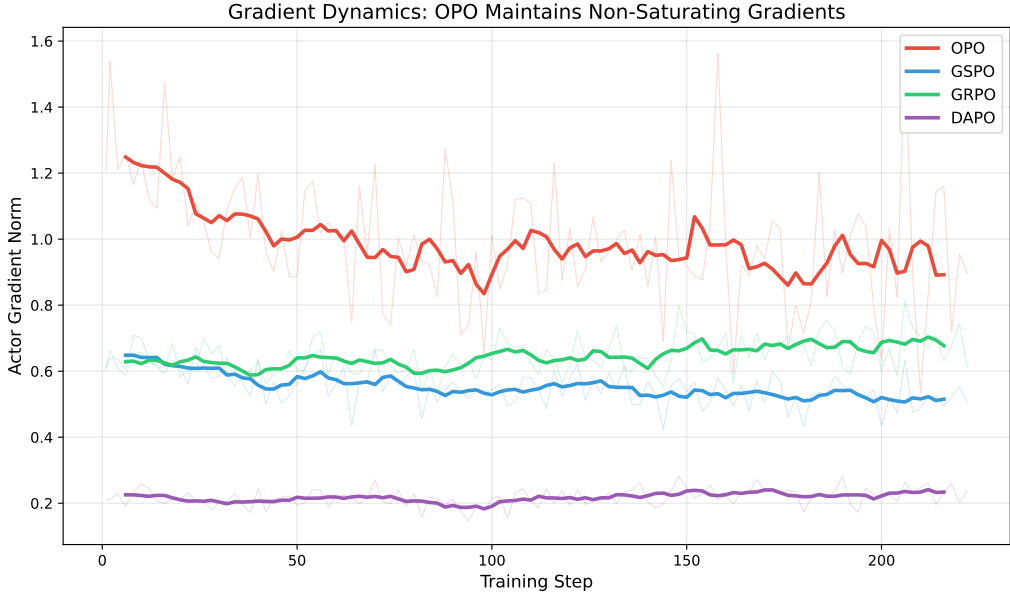


Figure 4: Gradient norm comparison. OPO maintains healthy gradient norms (0.9) throughout training, while DAPO (0.22) and GSPO (0.50) exhibit gradient decay.

**Entropy Dynamics.** Figure 5 depicts the policy entropy throughout training. OPO maintains consistently higher entropy levels compared to baselines. We attribute this to the granularity of supervision: GRPO and DAPO utilize **token-level** updates, imposing dense supervision that forces the policy to collapse rapidly into specific phrasings. In contrast, OPO (and GSPO) employs **sequence-level** updates. This “sparse” supervision aligns the total trajectory probability without micromanaging individual tokens, thereby preserving policy diversity and exploration potential.

**Summary of Findings.** The experimental results confirm that OPO’s orthogonalized design—combining  $\alpha$ -weighted sampling with  $\chi^2$  optimization geometry—prevents gradient saturation and enables continued learning in high-confidence regimes.

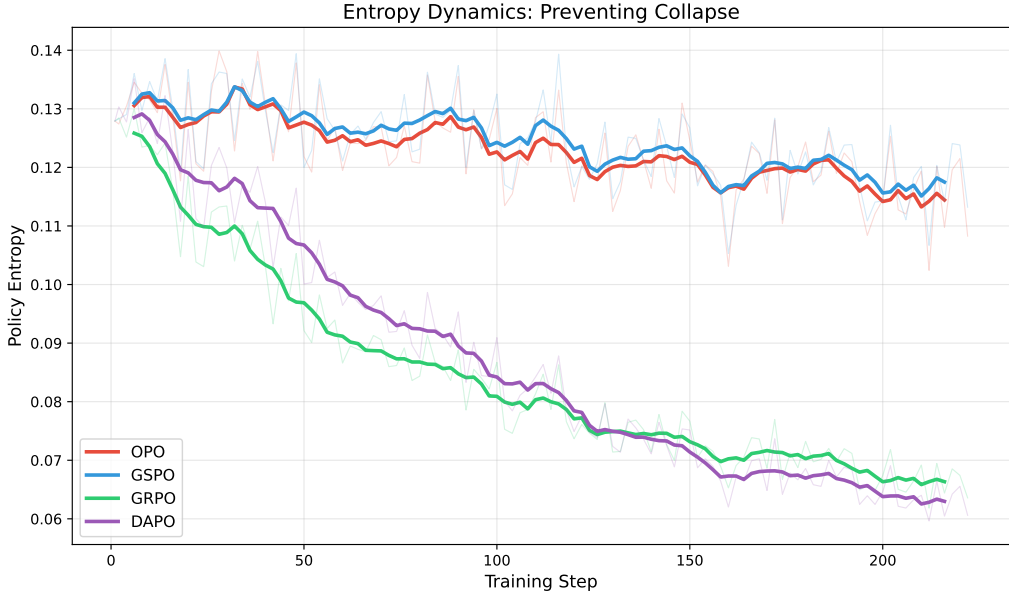


Figure 5: Entropy dynamics. OPO maintains higher entropy than baselines, preventing premature mode collapse and enabling sustained exploration throughout the training process.

## 7 Discussion

**Relation to Existing Methods.** OPO can be viewed as a generalization of existing alignment methods:

- Setting  $\alpha = 1$  and removing the quadratic term recovers SFT-like behavior.
- Setting  $\alpha \rightarrow 0$  and using KL geometry yields objectives with similar peak-seeking and exponential-type weighting effects as in KL-regularized preference optimization (e.g., DPO).
- OPO occupies the previously unexplored region of the design space: peak-seeking sampling with quadratic regularization in ratio coordinates.

**Computational Cost.** OPO incurs no additional model forward/backward passes compared to DPO/GRPO; the extra bookkeeping for  $\omega_\alpha$  is lightweight in practice.

**Role of the Reference Policy.** In OPO, the reference policy  $\pi_{\text{ref}}$  serves solely as an *origin* defining the coordinate system for the ratio  $v_\theta = \pi_\theta / \pi_{\text{ref}} - 1$ , rather than as an explicit regularizer via KL divergence. Stability is instead enforced by the quadratic penalty  $\frac{\mu}{2} v^2$ . This decoupling clarifies the distinct roles of anchoring (coordinate system) and regularization (optimization geometry).

**Implementation Notes.** The OPO objective (Equation (7)) involves expectations under  $\pi_{\text{ref}}$ . In practice:

- For on-policy training where samples come from  $\pi_{\text{ref}} = \pi_{\text{old}}$ , the batch itself provides an unbiased estimate.
- For off-policy settings, importance sampling or a separate reference sample set can be used.

**Limitations.** The framework introduces hyperparameters  $(\alpha, \mu)$  that may require tuning. Our experiments focus on reasoning tasks; validation on diverse domains (code generation, general instruction following) remains future work. Larger-scale experiments across diverse tasks and model sizes are needed to fully characterize the strengths and limitations of OPO.

## 8 Conclusion

We have presented **Orthogonalized Policy Optimization (OPO)**, a framework that decomposes alignment objectives into two independent design axes: sampling geometry and optimization geometry. By working in ratio coordinates where Pearson  $\chi^2$  divergence naturally induces quadratic penalties, OPO avoids the entangled dynamics of KL-based methods and provides a well-conditioned objective with linear gradient dynamics. Our analysis shows that OPO maintains stable optimization even in high-confidence regimes, addressing a key limitation of existing methods in reasoning tasks. We believe OPO provides a principled foundation for future work on robust and scalable LLM alignment.

## References

- [1] R. Rafailov, A. Sharma, E. Mitchell, S. Ermon, C. D. Manning, and C. Finn. Direct Preference Optimization: Your Language Model is Secretly a Reward Model. *NeurIPS*, 2023.
- [2] J. Schulman, F. Wolski, P. Dhariwal, A. Radford, and O. Klimov. Proximal Policy Optimization Algorithms. arXiv:1707.06347, 2017.
- [3] J. Schulman, S. Levine, P. Moritz, M. I. Jordan, and P. Abbeel. Trust Region Policy Optimization. *ICML*, 2015.
- [4] Z. Shao, P. Wang, Q. Zhu, R. Xu, J. Song, X. Bi, H. Zhang, M. Zhang, Y. K. Li, Y. Wu, and D. Guo. DeepSeekMath: Pushing the Limits of Mathematical Reasoning in Open Language Models. arXiv:2402.03300, 2024.
- [5] P. Christiano, J. Leike, T. B. Brown, M. Martic, S. Legg, and D. Amodei. Deep Reinforcement Learning from Human Preferences. *NeurIPS*, 2017.
- [6] L. Ouyang, J. Wu, X. Jiang, D. Almeida, C. L. Wainwright, P. Mishkin, et al. Training Language Models to Follow Instructions with Human Feedback. *NeurIPS*, 2022.
- [7] M. G. Azar, M. Rowland, B. Piot, D. Guo, D. Calandriello, M. Valko, and R. Munos. A General Theoretical Paradigm to Understand Learning from Human Preferences. *AISTATS*, 2024.
- [8] Y. Meng, M. Xia, and D. Chen. SimPO: Simple Preference Optimization with a Reference-Free Reward. *NeurIPS*, 2024.
- [9] I. Csiszár. Information-type measures of difference of probability distributions and indirect observations. *Studia Sci. Math. Hungar.*, 2:299–318, 1967.
- [10] S. M. Ali and S. D. Silvey. A General Class of Coefficients of Divergence of One Distribution from Another. *JRSS-B*, 28(1):131–142, 1966.
- [11] S. Amari. *Information Geometry and Its Applications*. Springer, 2016.
- [12] Y. Li and R. E. Turner. Rényi Divergence Variational Inference. *NeurIPS*, 2016.
- [13] S. Nowozin, B. Cseke, and R. Tomioka. f-GAN: Training Generative Neural Samplers Using Variational Divergence Minimization. *NeurIPS*, 2016.
- [14] S. K. S. Ghasemipour, R. Zemel, and S. Gu. A Divergence Minimization Perspective on Imitation Learning Methods. *CoRL*, 2020.
- [15] H. Xu *et al.* Improving Proximal Policy Optimization with Alpha Divergence. *Neurocomputing*, 2023.
- [16] Z. Wang. APO: Alpha-Divergence Preference Optimization. arXiv:2512.22953, 2025.
- [17] Z. Wang. ADPO: Anchored Direct Preference Optimization. arXiv:2510.18913, 2025.

## A Theoretical Proofs and Derivations

### A.1 Log-Ratio Approximation Error

**Lemma A.1** (Log-Ratio Approximation Error). *Let  $\Delta_\theta(y) = \log \pi_\theta(y) - \log \pi_{\text{ref}}(y)$  be the log-ratio, and  $v_\theta(y) = \exp(\Delta_\theta(y)) - 1$  be the exact ratio deviation. Let  $\delta = \|\Delta_\theta\|_\infty$ . For  $\delta < 1$  (trust region regime):*

$$|v_\theta - \Delta_\theta| \leq \frac{1}{2}\delta^2 e^\delta, \quad |v_\theta^2 - \Delta_\theta^2| \leq \delta^3 e^{2\delta} \quad (18)$$

*Consequently, the difference between the exact ratio loss and the log-approximate loss scales as  $O(\mathbb{E}[\Delta_\theta^3])$ .*

*Proof.* Using Taylor expansion  $e^x = 1 + x + \frac{x^2}{2} + \dots$ , we have  $v = \Delta + \frac{\Delta^2}{2} + O(\Delta^3)$ . The bounds follow from standard remainder estimation for the exponential function.

### A.2 Equivalence to $\chi^2$ -Constrained Maximization

**Proposition A.2** (Lagrange Dual Equivalence). *Consider the problem of maximizing alignment with the target  $\omega_\alpha$  subject to a functional  $\chi^2$  trust region:*

$$\max_{v \in L^2(\pi_{\text{ref}})} \mathbb{E}_{\pi_{\text{ref}}} [\omega_\alpha(y)v(y)] \quad \text{s.t.} \quad \mathbb{E}_{\pi_{\text{ref}}} [v(y)^2] \leq \epsilon \quad (19)$$

*The Lagrangian relaxation of this problem is exactly the OPO objective  $\mathcal{L}_{\text{OPO}} = -\mathbb{E}[\omega_\alpha v] + \frac{\mu}{2}\mathbb{E}[v^2]$ , where the regularization coefficient  $\mu$  is the Lagrange multiplier corresponding to the trust region radius  $\epsilon$ .*

The optimal solution is  $v^*(y) = \frac{1}{\mu}\omega_\alpha(y)$ . This duality implies that  $\alpha$  purely shapes the objective (alignment direction), while  $\mu$  purely enforces the feasibility radius (optimization geometry).

### A.3 Distributional Stability Guarantees

**Proposition A.3** ( $\chi^2$  Controls Total Variation). *Let  $TV(\pi, \pi_{\text{ref}}) = \frac{1}{2}\mathbb{E}_{\pi_{\text{ref}}} [|t(y) - 1|] = \frac{1}{2}\mathbb{E}[|v(y)|]$ . By Jensen's inequality:*

$$TV(\pi, \pi_{\text{ref}}) = \frac{1}{2}\mathbb{E}[|v|] \leq \frac{1}{2}\sqrt{\mathbb{E}[v^2]} \quad (20)$$

*Thus, bounding the  $\chi^2$  norm  $\mathbb{E}[v^2] \leq \epsilon$  guarantees that the policy remains within a  $\sqrt{\epsilon}/2$ -radius of the reference in Total Variation distance.*